



**NIST Advanced Manufacturing Series  
NIST AMS 100-46**

# **Design and Application of the Reconfigurable Mobile Manipulator Artifact (RMMA)**

Roger Bostelman  
Omar Aboul-Enein  
Soocheol Yoon  
Ya-Shian Li-Baboud

This publication is available free of charge from:  
<https://doi.org/10.6028/NIST.AMS.100-46>

**NIST Advanced Manufacturing Series  
NIST AMS 100-46**

# **Design and Application of the Reconfigurable Mobile Manipulator Artifact (RMMA)**

Roger Bostelman\*

*\*Former NIST employee; all work for this  
publication was done while at NIST.*

Omar Aboul-Enein  
*Intelligent Systems Division  
Engineering Laboratory*

Soocheol Yoon

*Intelligent Systems Division  
Engineering Laboratory  
Institute for Soft Matter  
Georgetown University*

Ya-Shian Li-Baboud

*Software and Systems Division  
Information Technology Laboratory*

This publication is available free of charge from:  
<https://doi.org/10.6028/NIST.AMS.100-46>

August 2022



U.S. Department of Commerce  
*Gina M. Raimondo, Secretary*

National Institute of Standards and Technology  
*Laurie E. Locascio, NIST Director and Under Secretary of Commerce for Standards and Technology*

NIST AMS 100-46  
August 2022

Certain commercial entities, equipment, or materials may be identified in this document in order to describe an experimental procedure or concept adequately. Such identification is not intended to imply recommendation or endorsement by the National Institute of Standards and Technology, nor is it intended to imply that the entities, materials, or equipment are necessarily the best available for the purpose.

### **NIST Technical Series Policies**

[Copyright, Fair Use, and Licensing Statements](#)

[NIST Technical Series Publication Identifier Syntax](#)

### **Publication History**

Approved by the NIST Editorial Review Board on 2022-08-15

### **How to Cite this NIST Technical Series Publication**

Bostelman R, Aboul-Enein O, Yoon S, Li-Baboud Y (2022) Design and Application of the Reconfigurable Mobile Manipulator Artifact (RMMA). (National Institute of Standards and Technology, Gaithersburg, MD), NIST Advanced Manufacturing Series (AMS) NIST AMS 100-46. <https://doi.org/10.6028/NIST.AMS.100-46>

### **NIST Author ORCID iDs**

Roger Bostelman: 0000-0003-3234-4345

Omar Aboul-Enein: 0000-0002-5361-4589

Soocheol Yoon: 0000-0002-1066-7867

Ya-Shian Li-Baboud: 0000-0002-8605-7758

### **Contact Information**

[omar.aboul-enein@nist.gov](mailto:omar.aboul-enein@nist.gov), 100 Bureau Dr. MS 8230, Gaithersburg, MD, 20899, 301-975-2703

## **Abstract**

Advancing the safety and performance of robotic arms onboard mobile robot bases, or mobile manipulators, requires accurate measurements. As mobile manipulators interact with a worktable or object, they require advanced measurement systems and test artifacts to evaluate how well they can perform tasks, such as assembly or inspection. Towards the standardization of measurement methods for the safety and performance of mobile manipulators, the National Institute of Standards and Technology (NIST) has developed a Reconfigurable Mobile Manipulator Artifact (RMMA) as a simulation of a worktable or object to characterize a mobile manipulator's ability to maneuver and meet its specified tolerances. The RMMA can be used to test key positioning capabilities for an assembly task execution, from a mobile manipulator's ability to register to the worktable followed by positioning its end effector to a series of assembly objects in a specified pattern. The RMMA includes fiducials with relatively low uncertainty, as compared to the mobile manipulator pose performance. The uncertainty of the mobile manipulator end-effector position was measured using a camera or a laser retroreflector sensor attached to the end-effector. The intent of developing the RMMA is for mobile manipulator manufacturers, users, and researchers to perform in-situ measurement during production or research for frequent system calibration. This paper describes the RMMA design and past RMMA metrology applications using an automatic guided vehicle (AGV) and a mobile robot, each supporting a six degree-of-freedom industrial robot arm, and RMMA/mobile manipulator ground truth measurement using an optical tracking system (OTS).

## **Keywords**

Automated guided vehicle; measurement artifact; mobile manipulator; mobile manipulator uncertainty; mobile robot; optical tracking system; reconfigurable mobile manipulator artifact; RMMA.

## Table of Contents

<b>1. Introduction</b> .....	<b>1</b>
1.1. Reconfigurable Mobile Manipulator Artifact (RMMA) .....	1
<b>2. RMMA Design</b> .....	<b>4</b>
2.1. Static-RMMA .....	4
2.2. Dynamic-RMMA .....	4
2.3. RMMA Components.....	5
<b>3. Development of mobile manipulator test methods</b> .....	<b>11</b>
3.1. Static-RMMA .....	13
3.2. Dynamic-RMMA .....	25
<b>4. Measurement Uncertainty</b> .....	<b>27</b>
<b>5. Conclusions</b> .....	<b>29</b>
<b>References</b> .....	<b>30</b>

## List of Tables

<b>Table 1.</b> Comparison of cart pose with the OTS measured data standard deviations. ....	20
<b>Table 2.</b> Results of the Cart Latch Variability Experiment.....	24

## List of Figures

<b>Fig. 1.</b> NIST reconfigurable mobile manipulator artifacts (RMMA): (a) Static-RMMA with adjustable height table with multiple geometric patterns of tapped holes; and (b) Dynamic-RMMA with flat (top/bottom), concave (inside edge), convex (outside edge) patterns of holes for mounting reflectors or laser retroreflectors and designed to mount into circular or sinusoidal shapes.....	2
<b>Fig. 2.</b> RMMA being used by a mobile manipulator with gripper (a) to insert a peg in a hole and (b) releasing the peg after insertion.....	3
<b>Fig. 3.</b> Static-RMMA Hole Plate design (in mm). ....	4
<b>Fig. 4.</b> Dynamic-RMMA Hole Plate design of the Curve Base (in mm).....	5
<b>Fig. 5.</b> Light Collimator Design. ....	6
<b>Fig. 6.</b> Reflector Screw Design.....	6
<b>Fig. 7.</b> Rotation-Top Design. ....	7
<b>Fig. 8.</b> Rotation-Bottom Design. ....	7
<b>Fig. 9.</b> Optional square reflector: a) adaptor and b) adaptor-to-circular hole converter.....	8
<b>Fig. 10.</b> Components positioned in order of their interconnects to other components and the Hole Plate from Figs. 5-9 CAD models. ....	9
<b>Fig. 11.</b> a) All components assembled and attached to the RMMA hole plate; and (b) close-up of the angled reflector components at 45° from the vertical axis. Note that the measurement experiments described in this paper did not use the optional rotation components. ....	10
<b>Fig. 12.</b> Laser retroreflector sensor (yellow and black) attached to a robot adaptor. (a) Collimator dimensions and laser retroreflector measurement distances and offsets. (b) Mobile	

manipulator aligned with fiducial (i.e., reflector fixed to the reflector screw). Spherical OTS markers are also shown attached to the laser retroreflector, robot, tool-mount, and the AGV (background)..... 11

**Fig. 13.** (a) AGV beside the Static-RMMA [6]. (b) AMR with robot arm mounted onboard [15]. (c) AMR-CT with robot arm mounted onboard a cart [18]. ..... 12

**Fig. 14.** AGV beside the Static-RMMA using Augmented Reality (AR) toolkit for registration.15

**Fig. 15.** Examples of the variety of mobile manipulator access poses with respect to the Static-RMMA that are possible for mobile manipulator performance measurement. The inset photo shows a closeup of the fiducials. .... 17

**Fig. 16.** RMMA setup with BFs (Large Reflector) near each AF (Small Reflector) and the Edge (Reflective) Tape [18]. ..... 18

**Fig. 17.** Side vs Registration Method Plots for Mobile Manipulator-on-a-Cart Experiment [18]. ..... 21

**Fig. 18.** OTS fiducial placement on the cart transporter vehicle (left) and cart payload structure base (center) for cart latch variability experiment. Corresponding OTS rigid bodies (right). 22

**Fig. 19.** Cart transporter vehicle parked at an arbitrary goal in front of cart (left) and corresponding vehicle map screenshot (right). ..... 22

**Fig. 20.** Marked tape used to manually re-center the cart position between trials for run 2. 23

**Fig. 21.** Plotted distance between the VEHICLE and CART Rigid Body Centroids for run 1 (top) and run 2 (bottom). ..... 25

**Fig. 22.** (a) Initial Marquette University Dynamic-RMMA; and (b) NIST Dynamic-RMMA used at Marquette University. .... 26

**Fig. 23.** Dynamic-RMMA used at NIST..... 27

**Fig. 24.** Summary of coordinate system calibrations for technology transfer that included a) 6DOF registration between the 2D AMR-CT vehicle map coordinate system and the OTS using  $i$  pose measurements of the vehicle base (denoted “vbase”), b) registration of the vehicle base to the vehicle frame (denoted “vframe”, and c) registration of the vehicle frame to the cart base (denoted “cbase”). Homogeneous transformation matrices between the specified source and destination coordinate frames are denoted  $H$ , with bolding indicating the unknown transformations that were solved..... 27

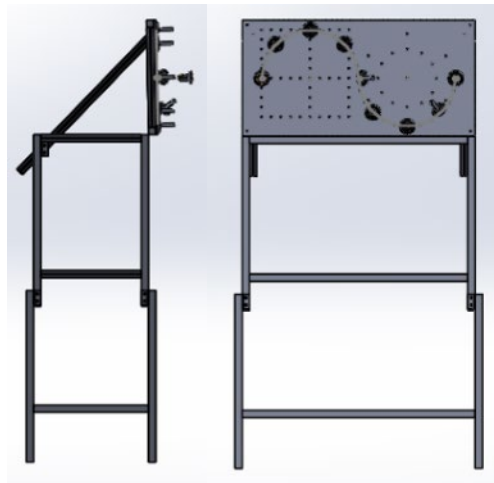
## 1. Introduction

With the increase in the use of mobile manipulators in several industries [1][2][3], the ability to measure mobile manipulator safety and performance has become critical. Many measurement systems [4] marketed today, include: optical tracking systems, laser trackers, and inertial measurement systems. They typically provide accurate positioning information at a relatively high cost to the needed measurements. Measurement artifacts that are machined or made using additive manufacturing technologies can provide useful safety and performance measurement information at a relatively low cost. The mobile manipulator measurement artifacts can assess positioning performance in situ and can be applied to relatively high accuracy applications such as assembly or inspection. Artifacts to test the performance of robot and mobile robot or Automatic Guided Vehicle (AGV) safety appear in their respective safety standards. For example, in Industrial Truck Standards Development Forum (ITSDF) B56.5, three artifacts or test pieces are described with their dimensions and surface coatings [5]. However, industrial safety system performance measurement artifact research is non-existent for robots. A literature search provided no results for artifact use in robot performance measurements and provided minimal results for mobile robots or AGVs [6]. Based on the prior literature review [6], the National Institute of Standards and Technology (NIST) addressed the metrology gap in the evaluation of mobile manipulators by developing a novel test artifact for mobile manipulators. The objective of the Reconfigurable Mobile Manipulator Apparatus (RMMA) test artifact is to simulate a worktable or object to an adjustable machined uncertainty and can be applied to evaluate the intrinsic, such as docking accuracy or precision, and extrinsic sources, such as environmental conditions, contributing to the mobile manipulator's performance uncertainty. Applications of the RMMA include evaluation of the manipulator positioning capabilities for an assembly task execution as well as a mobile manipulator's ability to register to the worktable followed by positioning its end effector to a series of assembly objects in a specified pattern while stationary to or dynamically moving along the worktable or object. Registration is an essential part of the mobile manipulator evaluation test procedure to allow for flexibility in establishing a reference frame to the worktable to begin the task. Therefore, registration and fiducial detection are described in the tests to guide users in optimizing the mobile manipulator alignment to the work area and ultimately the detection accuracy of the specified industrial manipulation tasks.

### 1.1. Reconfigurable Mobile Manipulator Artifact (RMMA)

There are two Reconfigurable Mobile Manipulator Apparatus's (RMMAs), shown as graphical depictions in **Fig. 1**, designed, built, and tested at NIST, and used for measuring the performance of mobile manipulators. The artifacts allow machined surfaces (flat as in **Fig. 1(a)** or flat (top) and convex/concave (edges) as in **Fig. 1(b)**) with patterned holes to position reflectors and to be tilted horizontally, vertically, or at any angle beside or above the mobile manipulator. Each reflector can be positioned perpendicular to the surface or at any pitch and yaw angle using additional components. A relatively inexpensive laser retroreflector sensor, wielded by the manipulator and positioned above and in-line with each reflector, can be used to measure manipulator position accuracy (within the laser and reflector tolerance), repeatability, detection, time for detection, efficiency of motion, dexterity, and autonomy. Many of these parameters

can be determined by measurement from one mobile base position. Additionally, travel distance coupled with dexterity and autonomy can also be measured using the apparatus by indexing or continuously moving the mobile base along or around the apparatus. Alternatively, the robot could wield a reflector while the apparatus houses laser retroreflector sensors, resulting in a much simpler robot interface, but with greater cost from additional lasers. In either case, non-contact performance measurements bear no risk of damage to the mobile manipulator during calibration.



(a) Static-RMMA



(b) Dynamic-RMMA

**Fig. 1.** NIST RMMAs: (a) Static-RMMA with adjustable height table with multiple geometric patterns of tapped holes; and (b) Dynamic-RMMA with flat (top/bottom), concave (inside edge), convex (outside edge) patterns of holes for mounting reflectors or laser retroreflectors and designed to mount into circular shapes.

The RMMA can be used statically, where the mobile manipulator remains stationary while detecting the reflective fiducials, or dynamically positioning a mobile manipulator to an artifact. The mobile manipulator performance for a simulated manipulation task is executed by posing the end of arm tool (EOAT) attached to the manipulator at specific locations above the RMMA to automatically detect reflective fiducials with known uncertainties. The performance test criteria can include the:

- Time to register the mobile manipulator to the artifact;
- Time to move from the registration points to the assembly points;
- Accuracy of assembly point detection;
- Repeatability of detecting the assembly points;
- Number of search steps equating to the initial distance from registration/assembly points; and
- Detection of reflectors with varying diameters.

The RMMA was designed primarily to emulate the positioning requirements of an assembly task, specifically the peg-in-hole insertion task (see 2). It does this by providing a set of precisely positioned mount points for reflective targets. The targets are detected using a non-contact, laser retroreflector sensor designed to detect the presence of retro-reflective targets in line with the laser beam. The sensor is mounted as the EOAT. A camera, with a light source, could instead be used as the detection sensor, especially with a larger diameter reflector or other target. For the laser retroreflector concept, no camera software algorithm was required as the laser retroreflector connects directly to one of the robot manipulator's digital inputs. The reflectors can have specific diameters depending upon the required uncertainty of their location. The targets are designed to determine if the manipulator positioning is accurate enough for successful peg-in-hole insertion. The RMMA provides a way to test and verify the performance of mobile manipulator systems without the use of more expensive 3D tracking systems [7].

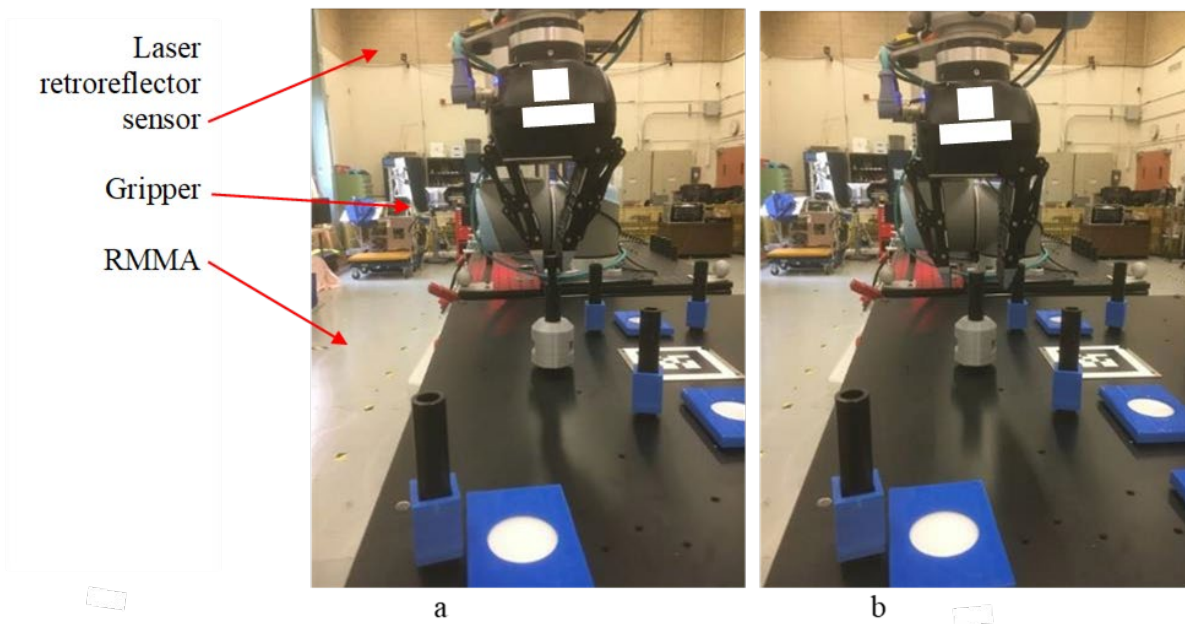


**Fig. 2.** Mobile manipulator with gripper (a) to insert a peg in a hole, and (b) releasing the peg after insertion.

## 2. RMMA Design

One of the two RMMAs, called the Static-RMMA, is used to simulate stationary mobile manipulator applications locating a worktable or object, such as an engine block and executing a manipulation task. Most tests performed to date have been with the Static-RMMA. The second RMMA design, called the Dynamic-RMMA, is used to simulate mobile manipulator applications that require continuous movement next to the worktable or object, such as when riveting or welding a long object. The Dynamic-RMMA, designed and built at NIST, was first tested at Marquette University followed by tests at NIST. These tests will be described in Section 3.2 Dynamic-RMMA. The following sections describe the design details for tests performed using both the Static-RMMA and the Dynamic-RMMA. The conclusions section summarizes the RMMA design and test process, as well as future planned tests.

### 2.1. Static-RMMA

The Static-RMMA hole plate design, shown in **Fig. 3**, includes a 12.7 mm thick x 1219.2 mm wide x 609.6 mm deep aluminum plate with several patterns of tapped holes machined into it to attach fiducials at known locations. The patterns include: two opposing semi-circles, a full circle, six squares, and a triangle. Components, as described in Section 2c RMMA Components, can be attached to the hole patterns for repeatable testing of known fiducial (e.g., reflector) poses.

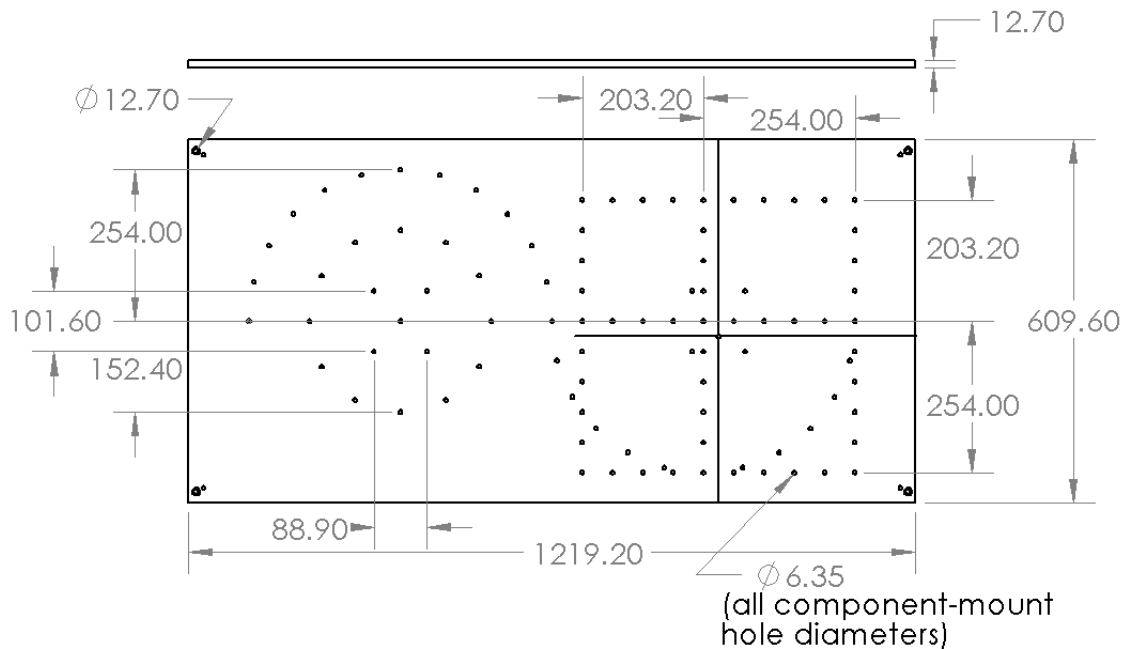


**Fig. 3.** Static-RMMA Hole Plate design (in mm).

### 2.2. Dynamic-RMMA

The Dynamic-RMMA hole plate design, shown in **Fig. 4**, includes an arc measuring 12.7 mm thick x 381 mm inside radius x 508 mm outside radius aluminum plate with several patterns of tapped holes machined into the top and arced surfaces to attach fiducials at known locations.

The holes are machined on the plate at a 444.5 mm and 15° increment spacing. The inside and outside radial edges are comprised of flat surfaces with tapped holes and flats machined to also attach fiducials, allowing the mobile manipulator to follow the assembly object along a path with concave and convex edges, respectively.

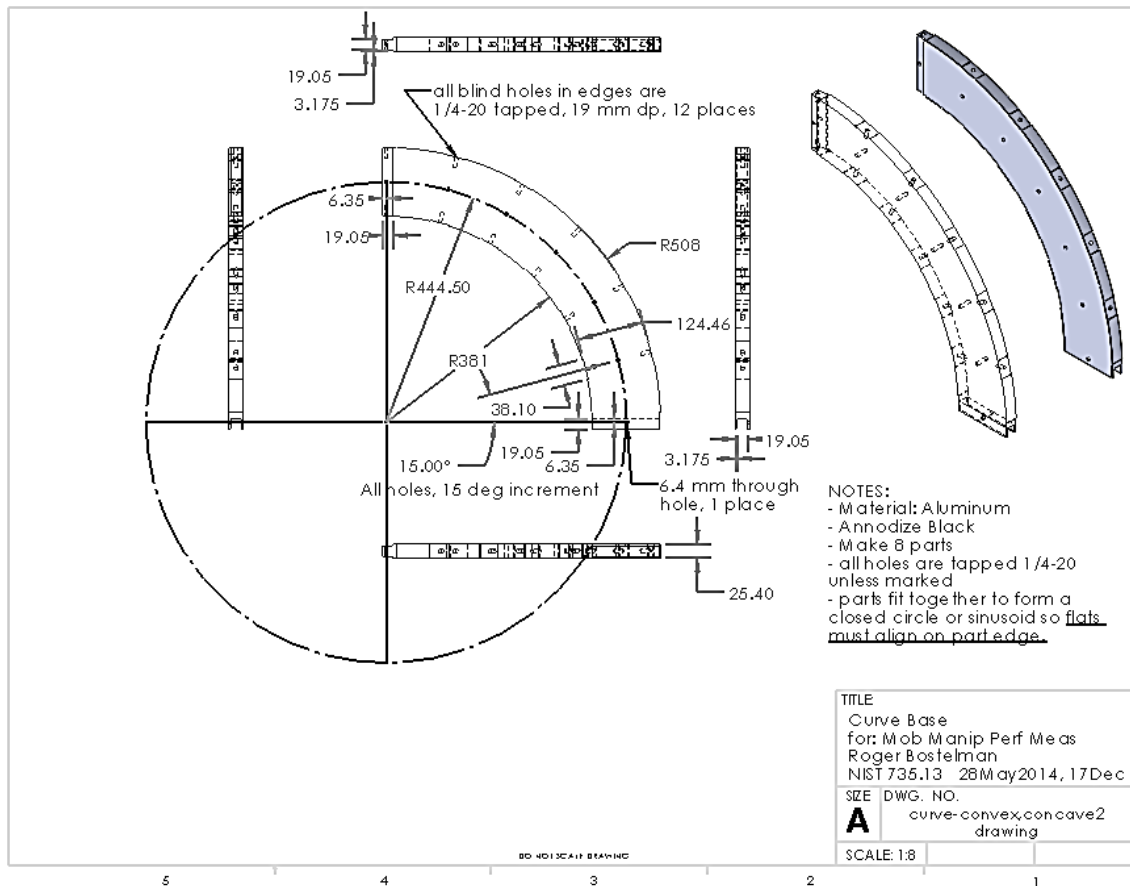
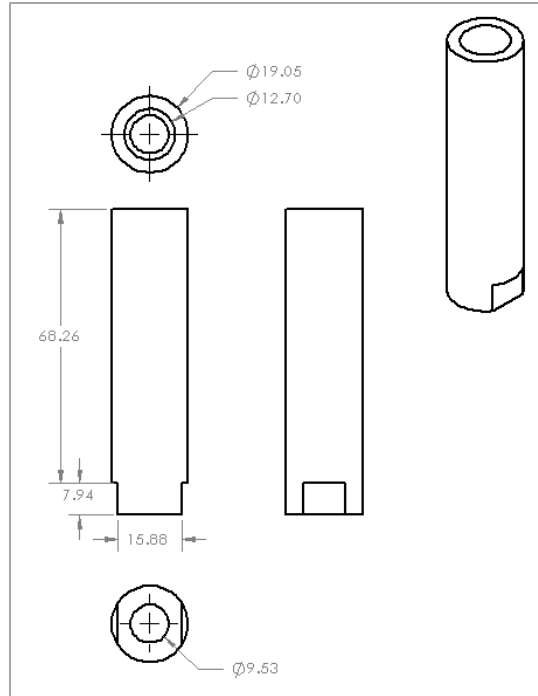


Fig. 4. Dynamic-RMMA Hole Plate design of the Curve Base (in mm).

### 2.3. RMMA Components

The RMMA components include: Light Collimator (see Fig. 5), Reflector Screw (see Fig. 6), Rotation-Top (see Fig. 7), and Rotation-Bottom (see Fig. 7). An optional square reflector adaptor-to-circular hole converter (see Fig. 9) was designed to allow off-the-shelf micro reflectors to be used. The components are attached together and to the Hole Plate as shown in the expanded assembly drawing in Fig. 10 and fully assembled as shown in Fig. 9. All components are machined out of black anodized aluminum.



**Fig. 5.** Light Collimator Design (in mm except as noted).

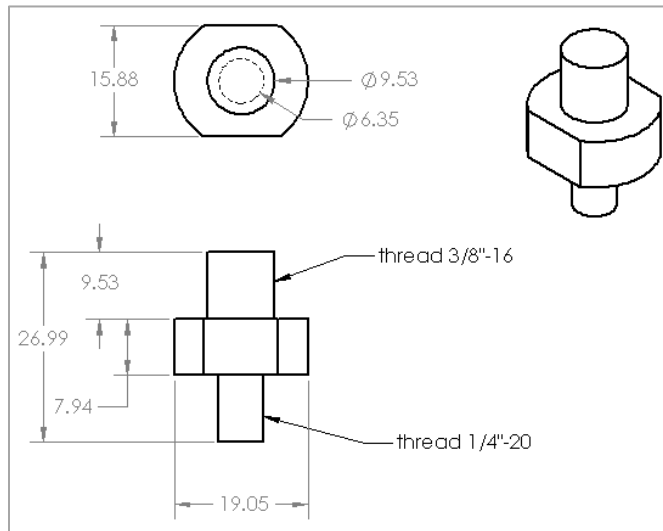


**Fig. 6.** Reflector Screw Design (in mm except as noted).

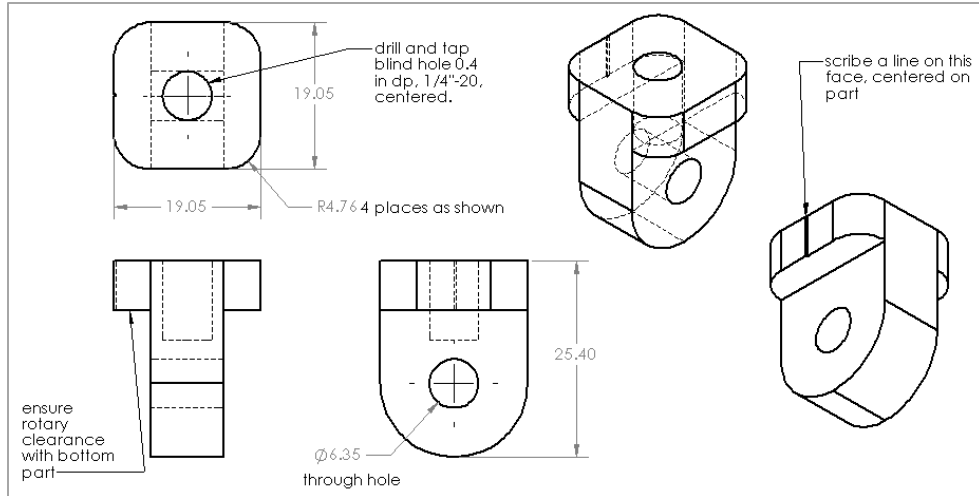


**Fig. 7. Rotation-Top Design (in mm except as noted).**

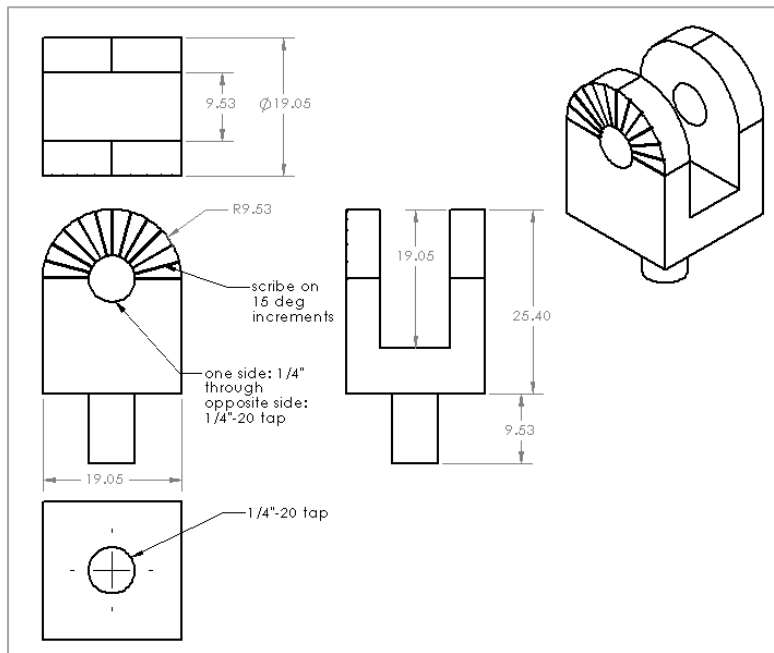


**Fig. 8. Rotation-Bottom Design (in mm except as noted).**

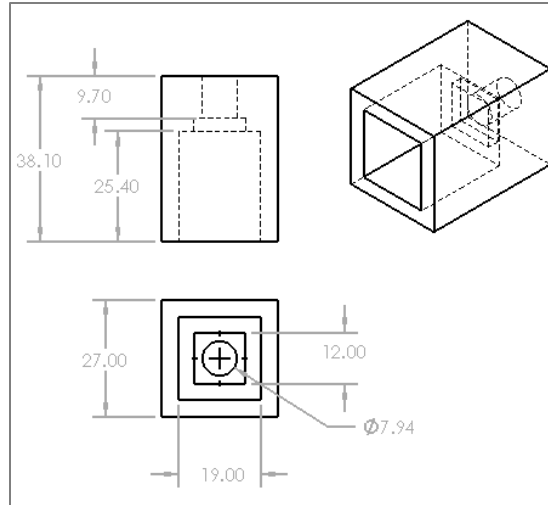


**Fig. 9.** Optional square reflector adaptor-to-circular hole converter (in mm).

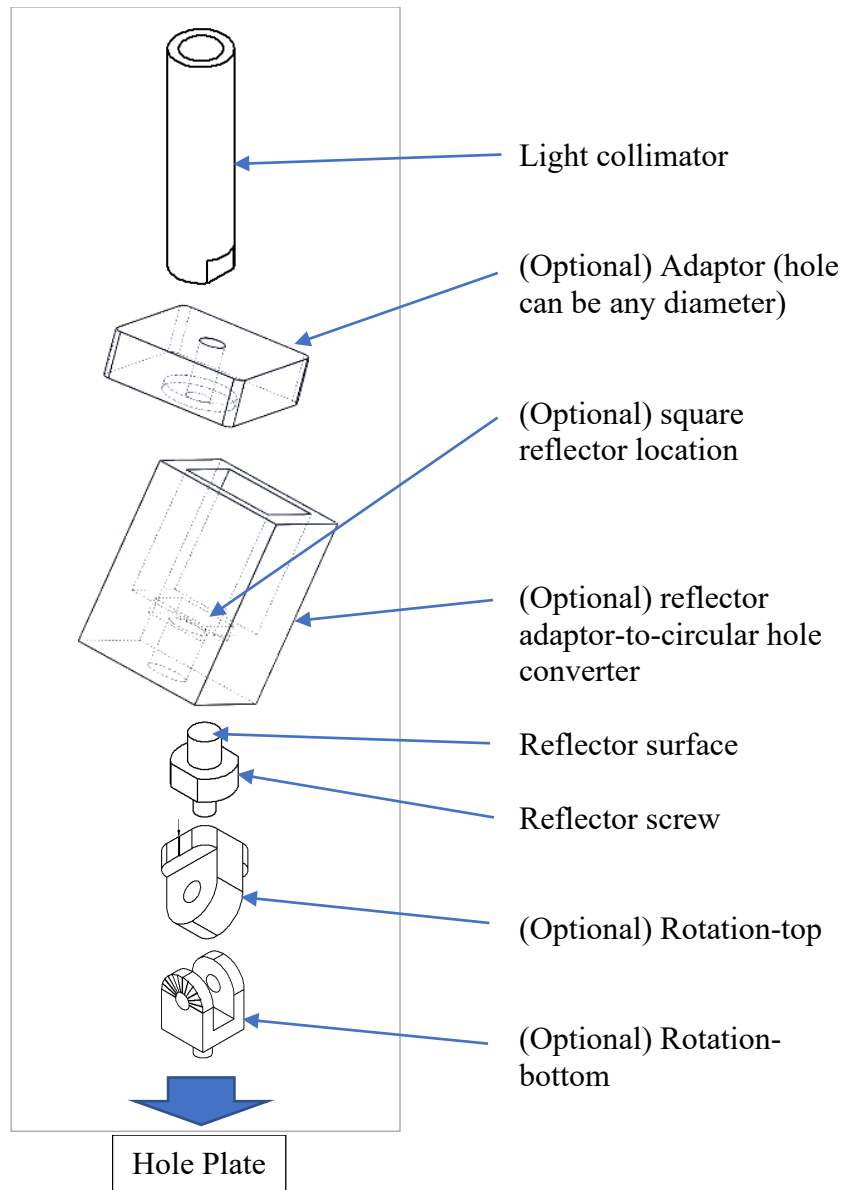


**Fig. 10.** Components positioned in order of their interconnects to other components and the Hole Plate from Figs. 5-9 CAD models.

**Fig. 10** shows all components, including the optional parts added to the light collimator and reflector screw. With the rotation components, the reflector and collimator can be rotated to pitch angles between  $\pm 90^\circ$  and yaw angles between  $0^\circ$  and  $360^\circ$ .

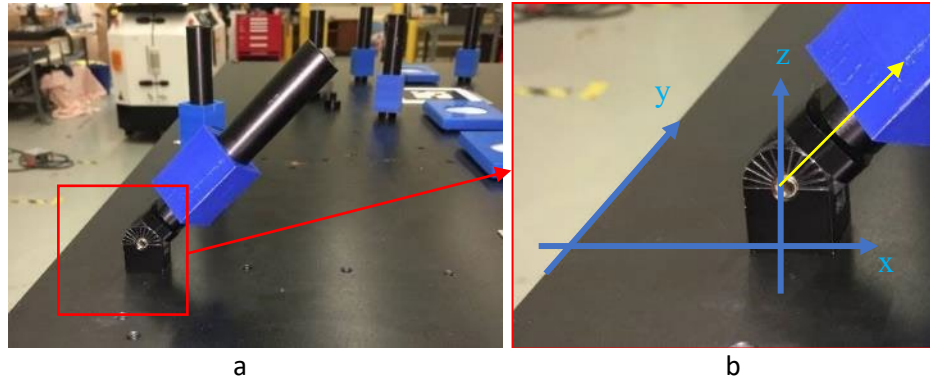


**Fig. 11.** a) All components assembled and attached to the RMMA hole plate; and (b) close-up of the angled reflector components at  $45^\circ$  from the vertical axis. Note that the measurement experiments described in this paper did not use the optional rotation components.

The RMMA could instead be made using additive manufacturing (as was used for the optional Adaptor and Reflector adaptor-to-circular hole converter) and is estimated to further reduce the artifact cost by another order of magnitude than an optical tracking system (OTS). However, dependent upon additive materials and processes, RMMA measurement uncertainty may increase.

The target fiducials are reflective material fixed to the reflector screw (see **Fig. 10**). The position of a reflector on the RMMA determines the mobile manipulator position relative to that reflector. As shown in **Fig. 11**, the rotation top and bottom are optional since alignment was tested only along the vertical axis.

The laser retroreflector sensor is used to detect the alignment of the manipulator with the fiducial. A signal is returned to the sensor when the laser beam is reflected back from the fiducial. The EOAT position accuracy can be evaluated by varying the size of the aperture or fixed radius used to expose the reflector. The smallest detectable reflector tested was 0.8 mm diameter. The tubular collimator is attached to the reflector screw to restrict the detection angle of the reflector as shown in **Fig. 12a**. **Fig. 12b** shows a mobile manipulator with laser retroreflector sensor aligned with the reflector screw within the collimator.

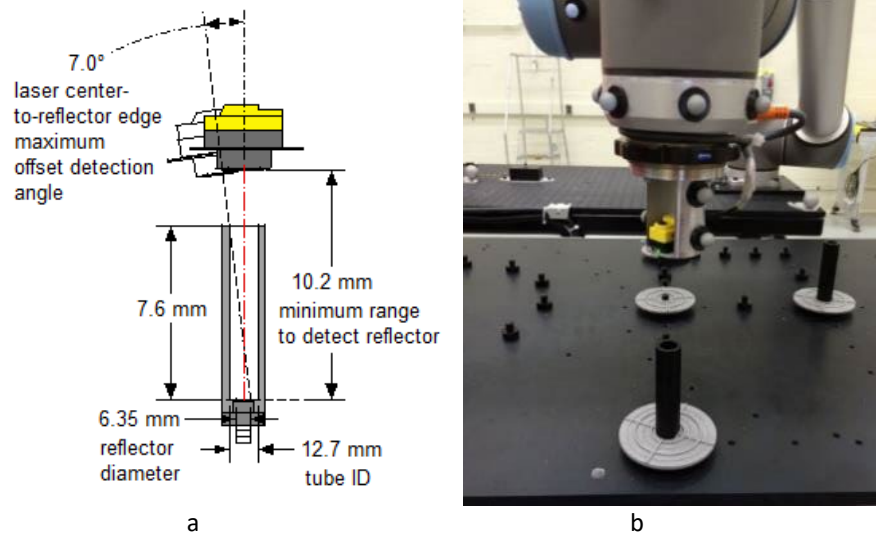


**Fig. 12.** Laser retroreflector sensor (yellow and black) attached to a robot adapter. (a) Collimator dimensions and laser retroreflector measurement distances and offsets. (b) Mobile manipulator aligned with fiducial (i.e., reflector fixed to the reflector screw). Spherical OTS markers are also shown attached to the laser retroreflector, robot, tool-mount, and the AGV (background).

The RMMA can be configured to be in horizontal, vertical, overhead, or at any angle between these configurations and at heights from relatively short to tall, as would be typical of assembly operations in, for example, automobile or aircraft manufacturing facilities. The RMMA legs can be changed to be shorter or taller.

For the NIST research, detector-to-reflector distance parallel to the laser axis was approximately 127 mm where the manufacturers specified minimum and maximum detection distances are 100 mm and 10 m, respectively. The distance researched would be representative of a programmed manipulator waypoint above and in-line with the next manipulator task point aligned to grip or insert a part or perform another task. The desired uncertainty may be, for example, a part insertion alignment tolerance required for a manufacturing assembly process. Moving along this grip or insertion line, parallel to the laser, at the aligned pose to the task point, also provides some knowledge of insertion performance (i.e., if the task point is continuously detected along the grip or insertion line).

### 3. Development of mobile manipulator test methods

Both the Static- and Dynamic-RMMAs were applied to a set of proposed test methods for testing mobile manipulator performance. In industry, it is expected that the RMMA would be used to verify mobile manipulator registration to the worktable and the alignment between the manipulator and task object. Registration is required since the mobile manipulator is not rigidly fixtured to the RMMA. Section 3 describes the registration and fiducial alignment tests performed at NIST. Upon registration, which should be as expeditious as possible to optimize productivity, testing the mobile manipulator alignment to the RMMA fiducials can commence. Alignment to fiducials simulates a typical scenario of robotic placement of pegs (e.g., rivets, drill bits) in holes or hole locations. Additionally, the alignment is a check on how well the

registration to the RMMA was initially performed. Hence, the various tests were intended to show how rapidly the mobile manipulator could navigate and dock with the Static-RMMA or navigate to and continuously navigate along the Dynamic-RMMA followed by using the RMMA to measure small fiducial alignment performance. The mobile manipulator did not “know” where the RMMA was positioned and oriented, and therefore required initial registration with the RMMA. Registration to the RMMA was followed by using the RMMA as a test artifact used to measure the mobile manipulator performance by aligning the end effector with the RMMA fiducials. The Static-RMMA was tested at NIST using the following three types of mobile manipulators:

- A. Automatic Guided Vehicle (AGV) ([6][8] [14] with an onboard 1300 mm long, 6 degree-of-freedom (6 DoF) robot arm (see **Fig. 13a**);
- B. Autonomous Mobile Robot (AMR) [17] with an onboard 850 mm long, 6 DoF robot arm (see **Fig. 13b**);
- C. Autonomous Mobile Robot - Cart Transporter (AMR-CT) [18] docked with and maneuvering a detachable cart with an onboard 850 mm long, 6 DoF robot arm robot arm (see **Fig. 13c**).

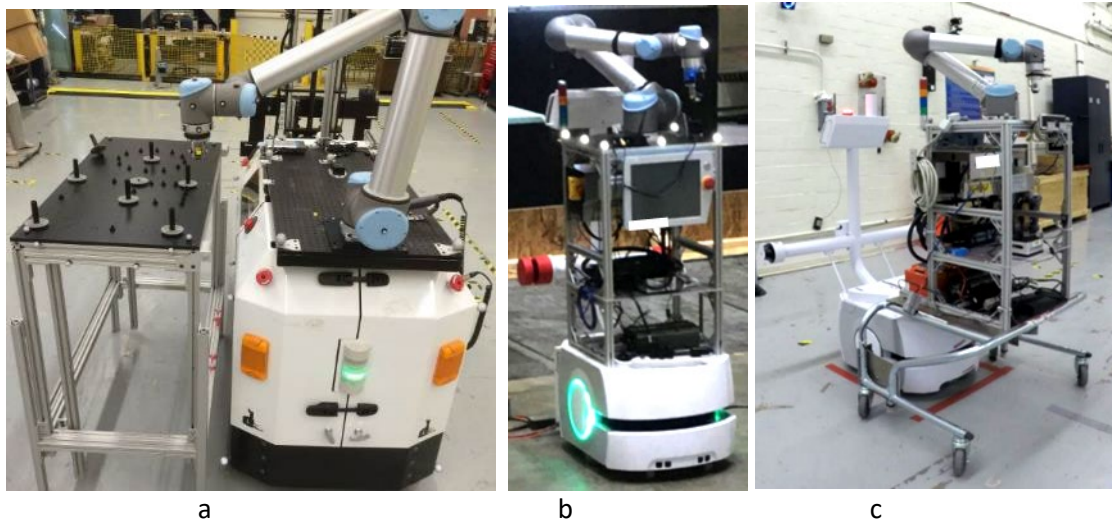


**Fig. 13.** (a) AGV beside the Static-RMMA [6]. (b) AMR with robot arm mounted onboard [17]. (c) AMR-CT with robot arm mounted onboard a cart [18].

The Dynamic-RMMA was tested at Marquette University using the AMR and at NIST using the AMR-CT.

The RMMA fiducials varied as follows:

- Assembly Fiducials (AF) - 0.8 mm to 6.4 mm diameter reflectors.
- Bisect Fiducials (BF) – 42 mm diameter reflectors.
- Augmented Reality (AR) Tags – marker system to support augmented reality tracking.
- Edge Tape – Multiple strips of 203.2 mm x 25.4 mm reflective tape along the RMMA edge.

Much of the experimentation was geared towards registration with the RMMA's fiducials as will be described in the next sub-sections.

### **3.1. Static-RMMA**

The Static-RMMA tests included a series of experiments that are labeled here using the A, B, and C mobile manipulator type labels from above. The tests describe the evolution of RMMA applications, starting with the Static-RMMA and only searching for fiducials for registration purposes. Beginning with A.3, registration was followed by AF detection and alignment as intended for both mobile manipulator registration and assembly performance measurement.

The tests with the AGV included:

- A.1) Registration using only a spiral search of AFs [6];
- A.2) Registration using only AR Tags [10]; and
- A.3) Registration using BFs followed by AF detection [10] [14][15].

The tests with the AMR included:

- B.1) Registration using BFs followed by AF detection [17].

The tests with the AMR-CT included:

- C.1) Registration using RMMA BFs and registration using edge-detection each followed by AF detection [18]; and
- C.2) An OTS experiment investigating potential variability in the cart latch.

This section will describe the Static-RMMA applications, including validation with the three mobile manipulator systems in sub-sections A.1 through C.2.

#### **A.1 AGV mobile manipulator - registration using only a spiral search of AFs**

An early experiment using the Static-RMMA tested the localization of 6.4 mm diameter AFs mounted to the RMMA in a square pattern [6]. The experiment focused on the measurement scenario in which the AGV repeatedly docked at approximately the same pose near the RMMA. On each stop, the manipulator performed a circular spiral search to detect four AFs 33 times. The step size gradually increased with the search radius and was initially set at half the diameter of the AF, or 3.1 mm [9]. The number of successful detects for each AF was recorded. In addition, total search times were recorded as well as when AF detection failed. The maximum number of fails in a single repetition was 15, with a total search time of 79.4 s in the test. The overall target detection rate was 93.23%.

The experiment included the scenario in which the AGV docked at six different poses next to the RMMA and detected two different AF patterns spaced 508 mm apart [9]. Three poses were near the circular pattern of six targets and the other three poses were near the square pattern of four AFs. In this experiment, the manipulator utilized the AGV pose for initial target search. This allowed the search algorithm to calibrate the transformation between the AGV and manipulator, as well as to adjust the initial search location of the two registration AFs based on the AGV docking pose. The manipulator performed detection of each AF 32 times at each of the six

poses. The number of detected AFs were recorded as well as the initial search steps to detect the AF. Search steps were counted as a measure of how far off from the fiducial that the manipulator was initially positioned and therefore required a search. As a result, the target detection rate was 97% or above, while the number of initial search steps varied from 73 to 1921 steps.

From the two tests, it was verified that the RMMA can measure the registration performance and repeatability performance of the AGV mobile manipulator without additional measurement systems. In addition, it was confirmed that the performance of the AGV mobile manipulator, according to the target location and AF pattern, as well as mobile base pose, can be measured using the RMMA. The AGV mobile manipulator was tested for performance stability and repeatability.

## **A.2 AGV mobile manipulator - registration using only AR Tags**

Augmented Reality (AR) marker-based tracking was applied to the AGV mobile manipulator to provide registration between the AGV and the RMMA in Ref. [10]. By extension, the AR software library could also track the docking pose of the manipulator base relative to the RMMA in six degrees-of-freedom. The experiment tested the mobile manipulator performance with the introduction of inter-system coordination between the AGV and the manipulator. Experiments were conducted on the AGV mobile manipulator system using A software Library for creating Virtual and Augmented Reality (ALVAR<sup>1</sup>), integrated with Robot Operating System (ROS) and using a 17 mm camera and 4.5 mm fixed focal length lens to track visual fiducials called “AR tags” (see **Fig. 14**) [10 - 13].

First, the static repeatability of the proposed tracking solution was tested on discrete intervals of its operating range or orientations. This was done by mounting a 200 mm x 200 mm target to a pan tilt mechanism inside of the camera view. The distance between the target and camera varied from 800 mm to 1000 mm across 26 unique positions and tilts. By taking 306 measurements within 30 s for each position, it was determined that the repeatability of the proposed tracking system was adequate for 11, OTS markers AGV mobile manipulator-to-RMMA registration since no measurement varied from the mean of any given position by more than 0.8 mm and the angular uncertainty was 0.18°.

The proposed AR tracking solution was successfully integrated with the AGV, and the AGV succeeded to dock with the RMMA as shown in **Fig. 15**. The camera was used to measure and communicate the AGV pose to the respective robot arm, which performed mock assembly on the RMMA square and circle patterns. These tests resulted in successful registration with the RMMA, although it was noted that the tracking solution, combined with other components of the system may have resulted in a larger overall error than with spiral searches on AFs. Therefore, future tests were suggested to combine AR based tracking with other laser-based search methods to reduce registration time [10].

Through this experiment, it was confirmed that the mobile manipulator performance applied with the AR visualization technology can be measured using the RMMA. Specifically, it was possible to measure the feasibility and performance of the registration method using markers and cameras.

---

<sup>1</sup> Disclaimer: Commercial equipment are identified in this paper to foster understanding. This does not imply recommendation or endorsement by NIST, nor that the equipment identified are necessarily the best available for the purpose.

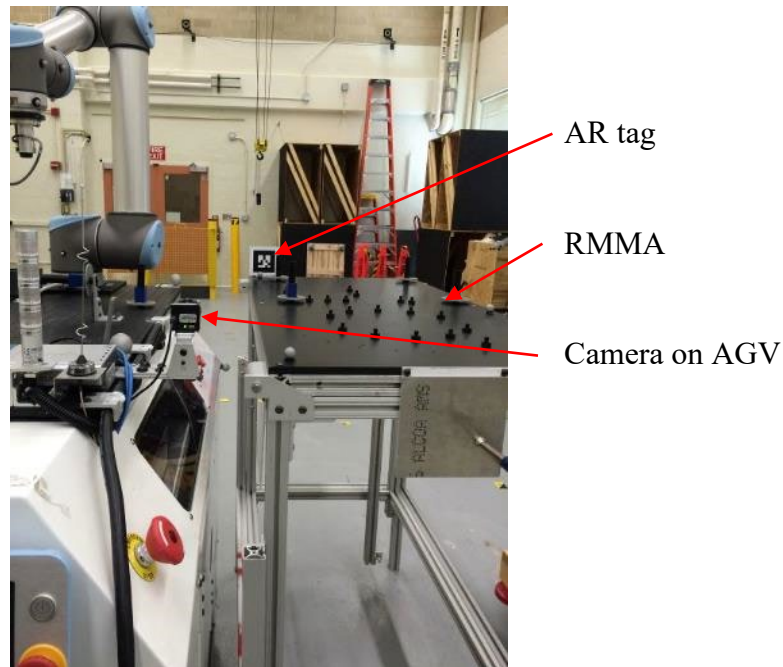


**Fig. 14.** AGV beside the Static-RMMA using Augmented Reality (AR) toolkit for registration.

### **A.3 AGV mobile manipulator - registration using BFs**

Using only spiral search as in A.1 for registration, the errors in the actual AGV docking position next to the RMMA could result in a lengthy initial registration [9]. A laser-bisection registration method was therefore introduced, in which the center of two BFs, per RMMA square or circle pattern, were detected to determine initial mobile base pose error [10]. If the mobile manipulator could determine the RMMA docking location more precisely using bisection, the registration performance would be improved. An additional square, fine (i.e., 0.5 mm step size) spiral search on two AFs after bisection proved to be more effective than only a spiral search in aligning the manipulator to the AFs.

In the first experiment, the bisect registration method was performed using 30 mm BFs. Following the laser bisection, a fine square spiral search on 1 mm diameter AFs was applied to re-register for more precise coordinate control. Then, the manipulator moved to and detected the remaining AFs in the square pattern. To compare the registration performance, 1 mm targets detection without bisect method were performed in advance. In summary, three sub-tests were conducted: 1) to detect the 1 mm diameter AFs using the square spiral search without bisection; 2) to detect the 1 mm diameter AFs using the spiral search after bisect registration; and 3) to detect AFs repeatably in the square pattern after the registration.

The success rate and the number of spiral search steps required to detect are measured for each test. For the first sub-test, 10 trials were conducted that resulted in a 91 % average success rate, 794 steps on average to detect the first AF and 12 steps on average to detect the second AF. For the second sub-test, a 92 % average success rate and 11 steps on average to detect the first AF and four steps on average to detect the second AF was observed. The number of search steps

required for the AFs represented an improvement over the first sub-test. For the third sub-test, which consisted of two 1 mm AFs and two 3 mm AFs on the square pattern and two 1 mm AFs and three 3 mm AFs on the circle pattern, were localized 32 times after performing the bisect registration. The average success rate (which excluded registration steps during bisection) was 98% to detect the AFs [14].

The second experiment was performed to compare a refined bisect method with the previous fine spiral search registration [10]. In this experiment, the RMMA was configured with reflective targets for both the circle geometric pattern, which used the 1 mm reflective targets, and the square geometric pattern, which used the 3 mm reflective target. The AGV was sent to six different poses next to the RMMA for five repetitions in which the manipulator would perform spiral search registration and then localize the remaining targets in the pattern while the AGV was stopped. It was found that the 3 mm AFs did not result in faster registration. The highest average number of search steps (869, or an average search time 360 s) was observed. The root mean square deviation (RMSD) was 776 steps (403 s). The same experiment was performed with the bisect registration method. The shorter registration time for the bisect method allowed for the AGV to instead cycle through 10 different poses per repetition instead of six. The average number of search steps after bisection was 1.8 (or an average search time of 0.8 s) and the RMSD number of search steps was 3.8 with a RMSD search time of 1.8 s. When the bisect method was utilized prior to the spiral search, the total time to register and localize targets after registration was 90 % faster than using the spiral search alone. This experiment demonstrated the efficiency and effectiveness of the bisect method for registration to the RMMA.

The most recent experiment with the AGV mobile manipulator was conducted to provide a complete set of publicly available experimental data for testing mobile manipulator systems with the RMMA and it was compared with an optical tracking system (OTS) used as ground truth [15]. The OTS data was captured in a volume with dynamic measurement uncertainties of 0.63 mm and  $0.57^\circ$  at the 95<sup>th</sup> percentile [16]. Like previous experiments, the AGV was programmed to travel between and stop at 10 different poses (see Fig. 15 for examples). The RMMA was outfitted with 2 mm diameter AFs in the square and circle patterns. The bisect registration method was performed using two 42 mm diameter BFs for each pattern. For each AGV pose, the manipulator was programmed to perform registration and then search AFs within a pattern using the square, fine spiral search.

The main outcome of this work was to document the experimental procedure, collected data and, anomalies with consideration for verifying RMMA measurements using ground-truth. In addition, anomalies that may occur when the AGV approaches the RMMA and their responses were observed and recorded.

Through those tests, it was confirmed that registration methods could be tested using the RMMA, and the difference in fiducial detection performance according to the registration method could be measured. In addition, it is possible to understand how the combination of the mobile manipulator pose and the registration method affects the fiducial detection performance. Furthermore, the influence of using the RMMA and its surrounding environment on the performance of the mobile manipulator can be confirmed. From a macroscopic point of view, factors that can affect the operation of the mobile manipulator can be identified using the RMMA. It is verified that 1 mm AF search performance can be measured through RMMA.

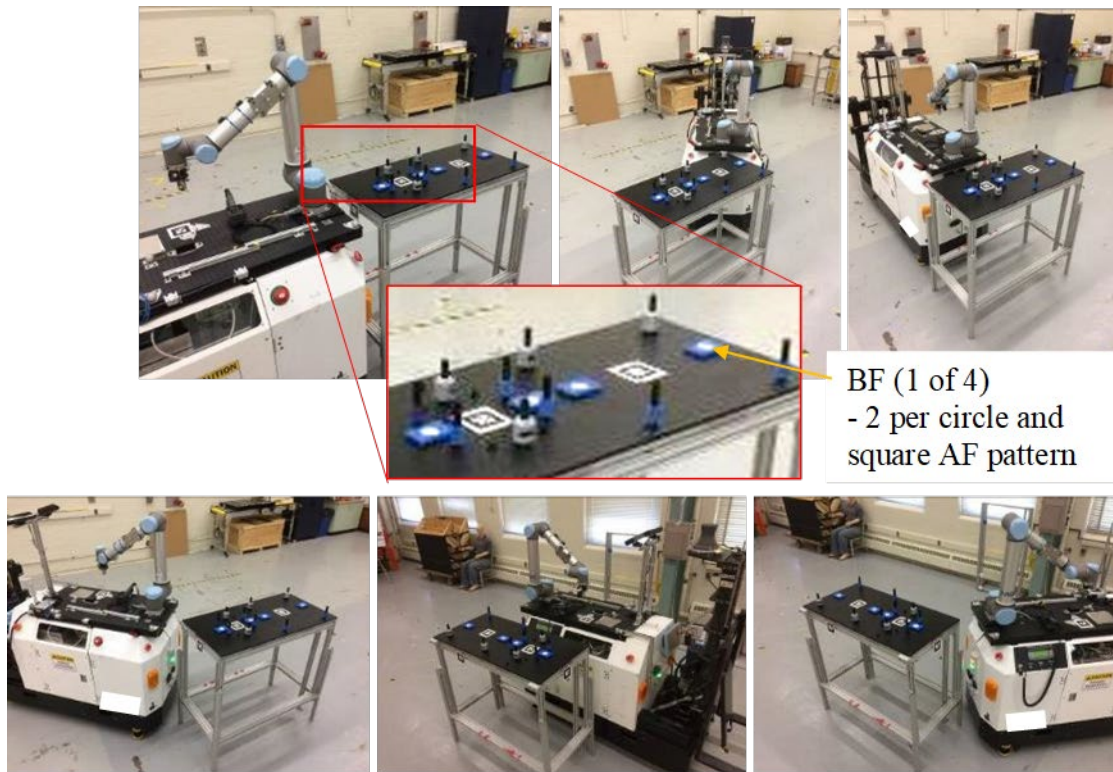


**Fig. 15.** Examples of the variety of mobile manipulator access poses with respect to the Static-RMMA that are possible for mobile manipulator performance measurement. The inset photo shows a closeup of the fiducials.

### **B.1 AMR mobile manipulator – fine search/bisect registration**

Following the experiments with the AGV, a test using the RMMA was conducted towards assessing the performance of an AMR mobile manipulator system [16]. In contrast to the AGV, the AMR navigates based on intelligent, autonomous route planning, localization, and obstacle avoidance using an environment map.

In this experiment, the RMMA square pattern was outfitted with four, 42 mm diameter BFs used for bisect registration and four, 2 mm diameter AFs (see **Fig. 16**). Due to the shorter reach of the smaller manipulator arm used with this system, the AMR alternatively navigated between and docked at two poses on either side of the square pattern. Then, the manipulator performed bisect registration and detection of the two AFs at each pose using spiral search. The test was performed 10 times including navigation, registration, and AF detection. A 10 mm-step-size spiral search was applied when the manipulator failed to detect the 42 mm target by its initial move [16].

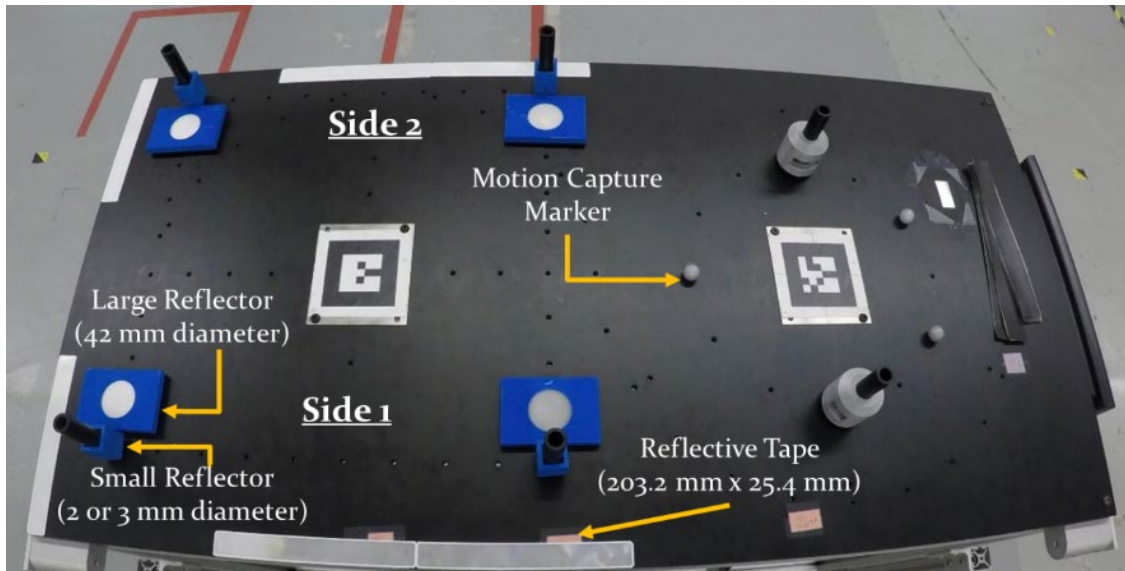


**Fig. 16.** RMMA setup with BFs (Large Reflector) near each AF (Small Reflector) and the Edge (Reflective) Tape [18].

During the experiment, the AMR pose, the search step of each manipulator moves, pose of manipulator EOAT, and task success rate were logged. The AMR showed docking pose errors of 22.6 mm in location and  $1.0^\circ$  in heading. This resulted in a propagated error in the EOAT position of 21.5 mm. Also, during registration, the manipulator performed 10 mm step-size spiral searches six times due to failed attempts to detect 42 mm target during its initial move. After registration two spiral searches were performed to detect the AFs. The mobile manipulator showed 21 mm uncertainty using the standard deviation of the first to second large reflector distances. The offset between the logged position of the AMR and the OTS measured position was found to be  $35.7 \text{ mm} \pm 5.4 \text{ mm}$ . The maximum difference of the measured EOAT position between the manipulator and the OTS was  $1.83 \text{ mm} \pm 1.0 \text{ mm}$ .

Through this experiment, it was confirmed that:

- the RMMA could be used to measure the performance of various mobile bases and manipulators;
- through the use of the RMMA and the experimental design process, it was confirmed that the manufacturing scenario should be adapted to fit the capabilities of the mobile manipulator (e.g., requiring the manipulator to stop at two sides of the RMMA because the arm was too short to reach both sides from a single location);
- a strategic search method is possible by selectively performing bisect registration and spiral search depending on the situation. (On the other hand, when compared with the mobile manipulator using the AGV and a larger manipulator, it was confirmed that the performance deteriorated in the initial move. This means that the RMMA can quantitatively measure the performance of various types of mobile manipulators); and
- using the RMMA, the mobile manipulator used in this experiment could successfully position relative to a 2 mm assembly target.

It was also shown that a precise level of mobile manipulator uncertainty can be measured when the OTS, a reference measurement system, is used. This means that not only the physical performance of the mobile manipulator, but also the sensor system, that is, the self-monitoring system performance can be measured using the RMMA [16].

### **C.1 AMR-CT mobile manipulator – edge and bisect registration**

A manipulator-on-a-cart maneuvered by a mobile base offers the potential benefits of increased flexibility, job concurrency, and hardware utilization, since the vehicle would be free to service other payloads while the manipulator, fixtured to a detachable cart, is occupied with an assembly task. It was hypothesized that new sources of performance uncertainty could be present in such systems that are not present in the AGV mobile manipulator or AMR mobile manipulator. For example, the manipulator-cart unlatching system (further discussed in C.2) and wheels may introduce inconsistent alignment between the cart and the RMMA that could impact the manipulator pose. Therefore, for this experiment, the RMMA was used to measure potential new sources of uncertainty in mobile manipulator-on-a-cart systems. Another improvement in this experiment was the introduction of an edge detection-based rapid coordinate registration method. Benefits to this new registration method include not requiring pre-recorded initial search points, as was the case with laser bisection, and a potentially faster registration time. Therefore, the experiment also statistically compared the speed and accuracy of the new edge registration to the previous bisect method [18].

For this test, the AMR-CT docked the manipulator-on-a-cart, similar to the AMR test, between two locations on either side of the RMMA square pattern. Also, for this test, two experiments were conducted: edge registration then bisect registration each followed by AF detection. A total of eight, 203.2 mm x 25.4 mm sized strips of retro-reflective tape, or Edge Tape, were mounted on each RMMA side and along the X and Y axes for the edge registration method (see **Fig. 16**). Additionally, as in B.1, two 42 mm diameter BFs and two 3 mm diameter AFs were mounted on each side of the RMMA square pattern. The AMR-CT docked next to each of the two sides of the square pattern six times on Side 1 and five times on Side 2 (see **Fig. 16**). for a total of 11 trials (or 22 observations between both the edge and bisect methods). Upon navigating to each sides' stop location, the vehicle unlatched from the cart (i.e., not contacting the cart) and paused. First, on each RMMA side, the manipulator performed the edge registration method followed by detection of two AFs using the square spiral search method. Then, staying at the same location, the manipulator performed bisect registration on two BFs again followed by detection of two AFs using the square spiral search method. The OTS was again used as a ground-truth reference for comparison with the mobile base and manipulator pose data [18].

Before analyzing the cart pose and the manipulator EOAT during the tests, a calibration was needed to find a coordinate transformation to express the OTS data, AMR-CT log data, and manipulator (coordinate registration and spiral search verification) log data in a common coordinate system. The distance between the calibrated log data and OTS data was between 0.025 mm and 2.6 mm for the EOAT and between 12 mm and 62 mm for the cart base. The result of comparing the standard deviations between the calibrated logged cart pose data and the OTS measured data is shown in **Table 1**.

**Table 1.** Uncertainty comparison of cart pose with the OTS measured data (standard deviations).

RMMA Side	Cart Pose	OTS
1	X: 25.8 mm Y: 13.0 mm 0.8°	X: 23.6 mm Y: 13.2 mm 0.8°
2	X: 43.8 mm Y: 15.4 mm 2.0°	X: 47.5 mm Y: 20.2 mm 2.0°

The standard deviation of the manipulator position, after detecting the 3 mm reflectors, was less than 2 mm as measured by both the OTS and the robot controller. Additionally, the measured AF separation distance (i.e., one side of the RMMA square pattern) using the manipulator EOAT, versus the 457 mm ground truth distance, was off between 5 mm and 14 mm, with a larger separation distance of 8 mm to 14 mm observed on Side 2 in comparison to Side 1, which exhibited a separation distance of 5 mm to 8 mm [18].

Comparisons of the sample registration time, number of spiral search steps to locate the first AF immediately after registration, and the corresponding initial-to-final spiral search distance are presented in **Fig. 17**. From **Fig. 17**, the lack of parallelism between the blue and orange lines, with the lines of **Fig. 17** (bottom-left) and **Fig. 17** (bottom-right) intersecting, suggested a possible interaction between measured RMMA side and coordinate registration method. From **Fig. 17** (top), it was observed that the sample registration time for the edge method was at least 2.5 times lower than the bisect method on both sides of the RMMA. In **Fig. 17** (bottom-left), it was observed that after registration the sample number of spiral search steps for the first AF was lower for the edge method than the bisect method on Side 1 of the RMMA, but the opposite was observed on Side 2 of the RMMA. This was similarly observed for the corresponding sample average initial-to-final spiral search distance in **Fig. 17** (bottom-right). Out of 11 bisect registrations, two required an initial coarse spiral search.

These coarse spiral searches both occurred on Side 2 of the RMMA and one resulted in the maximum registration time of 55 s. In contrast, the maximum registration time for the edge method was 22 s, which also occurred on Side 2 of the RMMA. Out of the 11 trials, the first AF was detected without requiring spiral search for one trial after performing edge registration and two trials after performing bisect registration. However, after the first AF was detected, the second AF was subsequently detected without requiring a spiral search for all trials with the edge registration. For the bisect method, the second AF was detected without requiring a spiral search for 9 out of the 11 trials. The two cases that a spiral search was required to find the second AF for the bisect method both occurred on Side 2 of the RMMA, with the spiral search requiring 5 and 15 search steps, respectively [18].

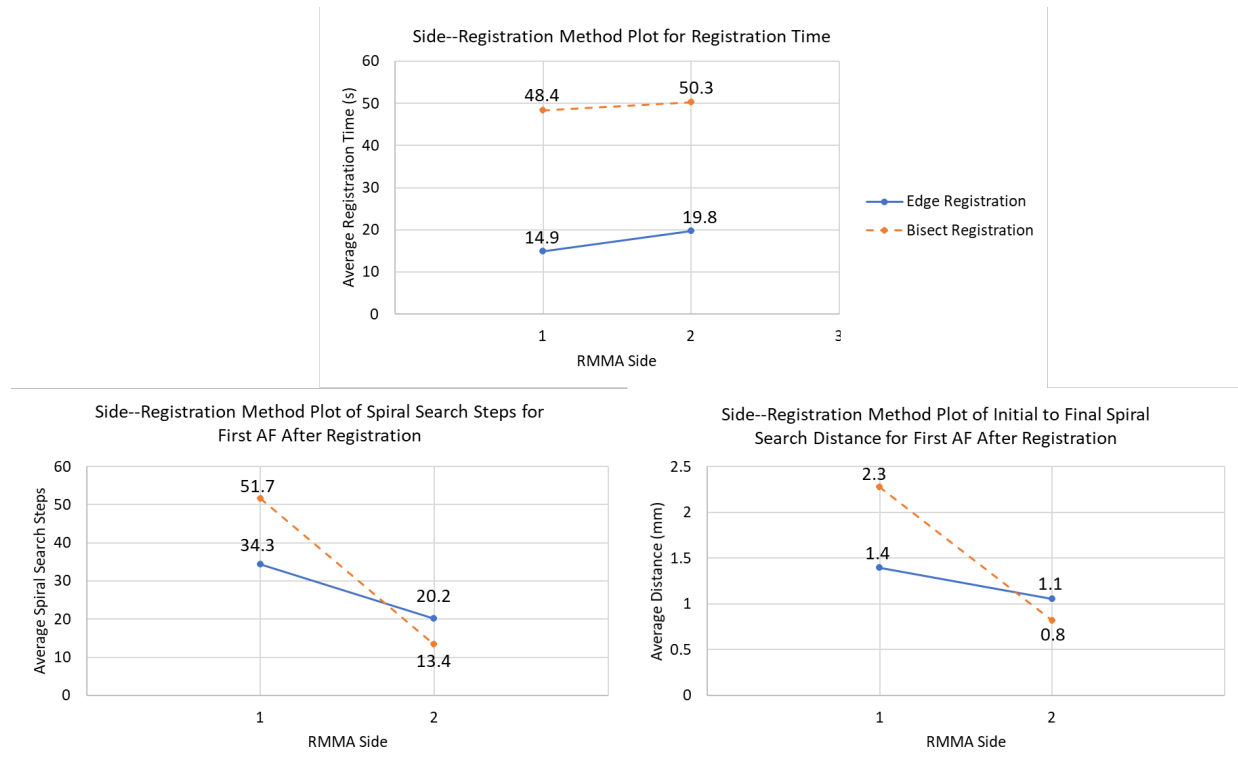


**Fig. 17.** Side vs Registration Method Plots for Mobile Manipulator-on-a-Cart Experiment [18].

### C.2 AMR-CT mobile manipulator – cart latch variability experiment

To provide further support for the presence of additional sources of uncertainty in the AMR-CT system that could affect alignment between the AMR-CT system and the RMMA, a simple experiment was performed with the same AMR-CT and OTS from Ref. [18] to measure any potential variability in the cart latching system. As depicted in **Fig. 18**, two rigid bodies were constructed from a total of 11 OTS markers with 19 mm diameter that were placed in asymmetric patterns on the cart transporter vehicle and cart payload structure base of the AMR-CT [18][20]. Note that the rigid bodies were labeled “VEHICLE” for the cart transporter vehicle and “CART” for the cart payload structure base. In total, two runs, each consisting of 10 trials, were performed to test the cart latch variability. The test procedure of run 1 differed only slightly from run 2, as will be described below. The OTS was re-calibrated immediately prior to each run using the manufacturer-specified procedure [21]. The OTS Motive software (version 2.2, see Ref. [22]) reported the calibration quality as “exceptional” for both runs, with a mean error of 0.633 mm and 0.618 mm for run 1 and run 2, respectively. For each trial of both runs, the vehicle was first sent to an arbitrary goal point placed in front of the cart and commanded to dock with the cart (see **Fig. 19**). Once the cart was latched, the position of both OTS rigid body centroids were recorded in a single, 10 s capture and exported in Comma Separated Value (CSV) format. Before starting the next trial, the position of the cart transporter vehicle was then reset by sending the vehicle back to the same initial goal point. Unlike run 1, where the position of the cart was not re-centered between trials, an operator manually re-centered the cart position between trials for run 2 using marked tape placed on the floor, as shown in **Fig. 20**.

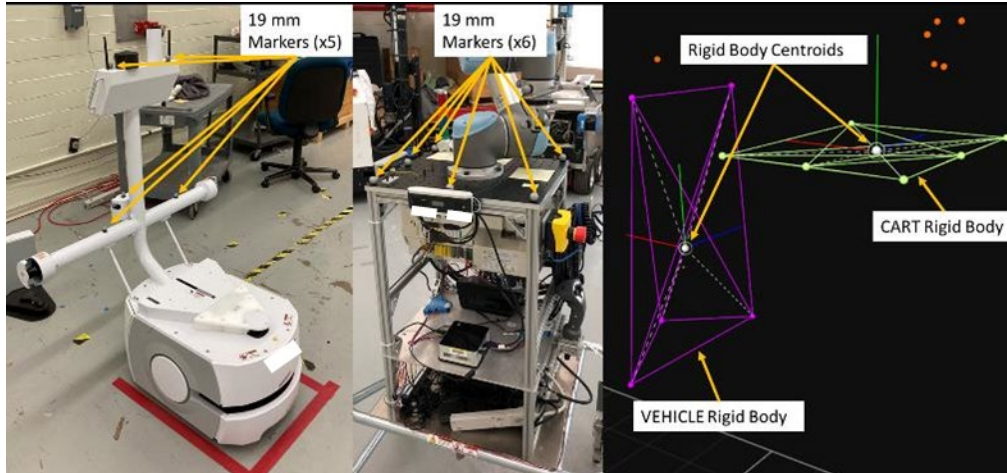


**Fig. 18.** OTS marker placement on the cart transporter vehicle (left) and cart payload structure base (center) for cart latch variability experiment. Corresponding OTS rigid bodies (right).

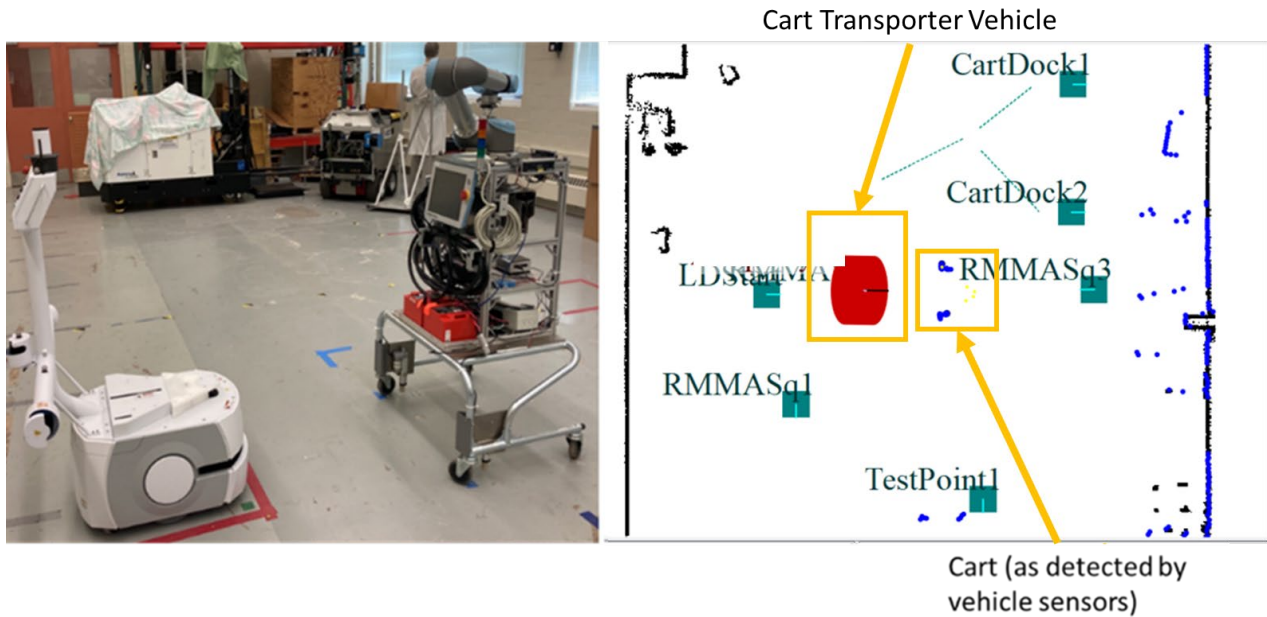


**Fig. 19.** Cart transporter vehicle parked at an arbitrary goal in front of cart (left) and corresponding vehicle map screenshot (right).



**Fig. 20.** Marked tape used to manually re-center the cart position between trials for run 2.

The exported CSV files were processed using Pandas version 1.2.4, a data analytics library, and Anaconda version 4.10.1, a Python distribution [23][24][23][24]. For each trial, the position components of the rigid body centroids along the X, Y, and Z axes were each averaged over the 10 second data capture interval at 120 frames per second for each trial. The average position components were then used to compute the Euclidean distance (in mm) between the VEHICLE and CART rigid body centroids. The Euclidean distance between rigid body centroids for each trial, as well as an average, standard deviation, and range distance are presented in **Table 2**. **Fig. 21** plots the computed Euclidean distance across trials for both runs.

From the results of run 2 in **Table 2**, negligible, sub-millimeter variability was observed in the alignment between the cart transporter vehicle and cart base when the position of the cart was manually re-centered between trials. However, from the results of run 1 in **Table 2**, a small, but more notable variability in distance was observed on the order of 1 mm for the standard deviation and up to about 3.6 mm for the range. In examining **Fig. 21**(top), a drift in the observations for run 1 was discerned as the trials progressed. This contrasted with **Fig. 21** (bottom), in which no consistent drift in the observed distances could be discerned across the trials of run 2. Since the only known difference between the two runs was the practice of re-centering the cart position, this suggested that the variability in the alignment of the latched cart with the cart transporter vehicle could be affected by external factors, such as floor level variability in different lab locations. In summary, this experiment demonstrated that the cart latch system of the AMR-CT could be affected by external factors to introduce additional position uncertainty between the cart transporter vehicle and manipulator base.

**Table 2.** Results of the Cart Latch Variability Experiment

	Euclidean Distance between VEHICLE and CART OTS Rigid Body Centroids (in mm)	Euclidean Distance between VEHICLE and CART OTS Rigid Body Centroids (in mm)
Trial	Run 1	Run 2
1	622.7309	623.1154
2	623.7798	623.5081
3	624.3458	623.1348
4	624.6725	622.8626
5	625.0952	622.5576
6	624.9183	623.2022
7	625.3577	623.2954
8	625.4186	622.9863
9	626.0315	623.2192
10	626.3078	623.1067
Mean	624.8658	623.0988
Stdev	1.0586	0.2570
Range	3.5769	0.9505

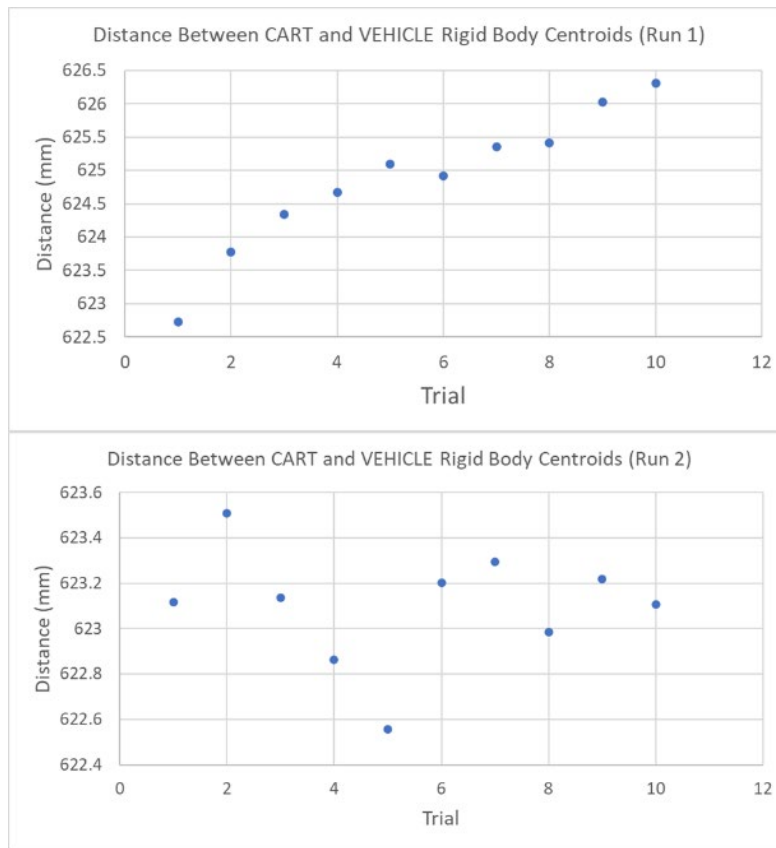


**Fig. 21.** Plotted distance between the VEHICLE and CART Rigid Body Centroids for run 1 (top) and run 2 (bottom).

### 3.2. Dynamic-RMMA

The Dynamic-RMMA, shown in **Fig. 1b**, was provided to Marquette University as part of NIST grants, entitled “Dynamic Performance Measurement of Mobile Manipulators” and “Performance Measurement of Mobile Manipulators using Coarse-to-Fine Deep Learning Methods”<sup>2</sup>.

The initial study reviewed the concept of continuous mobile manipulator movement while accessing preliminary Dynamic-RMMA fiducials (see **Fig. 22**). Results were published in [22] which analyzed “the problem of dynamically evaluating the positioning error of mobile manipulators.” In particular, the study “investigated the use of Bayesian methods to predict the position of the end-effector in the presence of uncertainty propagated from the mobile platform” where “precision of the mobile manipulator was evaluated through its ability to intercept retroreflective markers using a photoelectric sensor attached to the end-effector” similar to tests described in sections A1 and B1. Conclusions for their dynamic tests were described as “compared to a deterministic search approach, we observed improved robustness with comparable search times, thereby enabling effective calibration of the mobile manipulator.”

<sup>2</sup> NIST grant numbers 70NANB16H196 from 8/1/2016 – 8/30/2018 and 70NANB18H259 from 09/01/2018 – 08/31/2021 to Marquette University.

Two dynamic search mechanisms were used to locate fiducial markers using the mobile manipulator and laser retroreflector sensor method: a spiral-based deterministic method and a stochastic mechanism based on Kalman filters using the RMMA. Test results concluded that the stochastic approach intercepted 4.1 fiducials on average versus 3.9 from the spiral search method. The average search times were 4.2 s and 5.1 s, respectively.

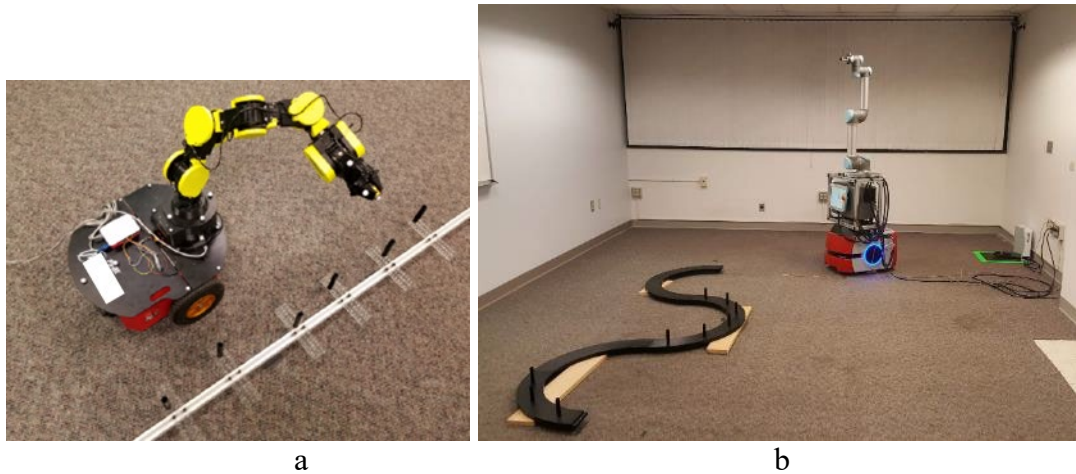


**Fig. 22.** (a) Initial Marquette University Dynamic-RMMA; and (b) NIST Dynamic-RMMA used at Marquette University.

Upon development of search methods using the initial Dynamic-RMMA, the actual Dynamic-RMMA (see **Fig. 22b**) was used at NIST to continue the Marquette University study. The mobile manipulator control algorithms developed at Marquette were transferred to NIST where researchers integrated the algorithms on the AMR-CT mobile manipulator (see **Fig. 23**). Activities to facilitate this transfer included the following: 1) establishing and troubleshooting an alternate development and simulation environment to account for differences in computer operating systems and 2) writing new code to interface directly with the AMR-CT vehicle through cleartext commands (since the on-board vehicle navigation of the AMR-CT replaced a separate navigation stack used for the Marquette mobile manipulator). Additionally, three calibration experiments were conducted to construct an alternate model of the AMR-CT mobile manipulator needed by the existing code base. An alternate model was required as NIST used a different vehicle and had a different payload structure causing a need for new transformations to be measured or calibrated using the OTS. These experiments included 1) the cart latch variability experiment described in Sec. 3.a.C.2, a calibration to register the 2D AMR-CT map coordinate system with the 3D OTS coordinate system, which was used as a global coordinate system (see **Fig. 24a**), and OTS measurements to establish transformations between the AMR-CT vehicle base and the base of the AMR-CT manipulator (see **Fig. 24b** and **c**). Results of the NIST technology transfer study are preliminary at this publication date.



Fig. 23. Dynamic-RMMA used at NIST.

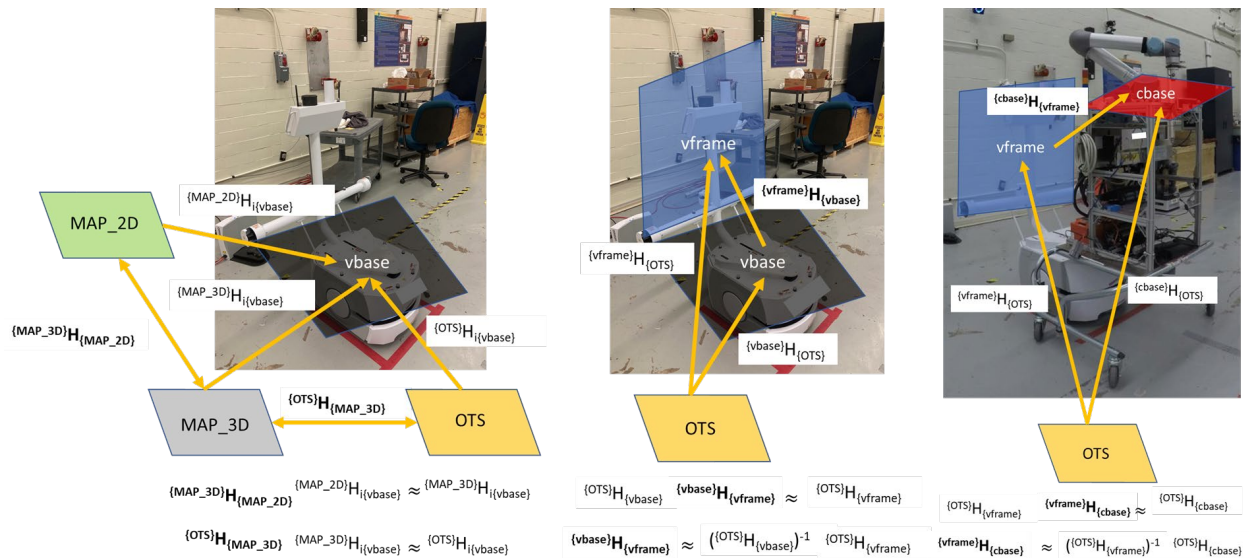


Fig. 24. Summary of coordinate system calibrations for technology transfer that included a) 6DOF registration between the 2D AMR-CT vehicle map coordinate system and the OTS using  $i$  pose measurements of the vehicle base (denoted “vbase”), b) registration of the vehicle base to the vehicle frame (denoted “vframe”, and c) registration of the vehicle frame to the cart base (denoted “cbase”). Homogeneous transformation matrices between the specified source and destination coordinate frames are denoted  $H$ , with bolding indicating the unknown transformations that were solved.

#### 4. Measurement Uncertainty

In addition to measuring the performance of the mobile manipulator, the RMMA can be used to measure the uncertainty of the related systems and environments. This section first describes

system uncertainties measured through a series of experiments. Then the sources of remaining measurement uncertainties and RMMA design factors to cope with them will be discussed.

In the experiments, the OTS was used as a reference measurement system, and for this, uncertainty of the OTS was measured first with the manufacturer's camera calibration wand (i.e., not the RMMA). The manipulator, as measured by the OTS, was observed to have static positional uncertainty of 0.022 mm and a dynamic uncertainty of 0.26 mm relative to the target fiducial. The corresponding angular uncertainties were  $0.023^\circ$  (static) and  $0.10^\circ$  (dynamic) [16]. Note that in this experiment, uncertainty was based on the standard deviation at 68% confidence [26].

Next, we measured the uncertainty of the mobile manipulator positioning, i.e., the mobile base localization and the manipulator EOAT positioning. Since the mobile manipulator determines the task parameters according to the data from the mobile base localization in real time, the localization uncertainty is an important factor which directly affects the task performance. The AMR showed a 35.7 mm positional uncertainty and  $1.7^\circ$  angular uncertainty in its localization. The manipulator showed an insignificant positional uncertainty. Instead, the travel distance of the manipulator, when the mobile base was parked next to the RMMA, was measured using two fixed points separated by 457.2 mm on the RMMA (i.e., one side of the RMMA square pattern of AFs). While the OTS logged 457.6 mm average AF separation distance, the manipulator logged 455.9 mm, a difference of 1.8 mm [17].

The RMMA can be used to measure the registration and assembly target repeatability and positioning uncertainties as demonstrated in tests methods with the AGV, AMR, and AMR-CT. However, several sources of measurement uncertainty in the experimental procedure and subsequent data analysis remain:

- misalignment between the mobile base and manipulator base centroids;
- mobile base orientation misalignment with the RMMA;
- mobile manipulator instability;
- OTS marker placement;
- uncertainty in the 3D printed reflective target fixtures; and
- data temporal alignment errors due to wireless transmission delay variability.

The sources of uncertainty may be acceptable since the RMMA was designed to reflect a realistic task, and the errors are within manufacturing tolerances for many types of assembly tasks. The RMMA and the performance measurements obtained by using it are focused on the mobile manipulator use-case (i.e., assembly). The RMMA was therefore designed and manufactured with machining tolerances typical of gear assembly, screw insertions, and metal or plastic pegs inserted into assemblies (i.e., in automotive body assemblies). These assembly uncertainties can be similar to machining tolerances of the RMMA surface and parts, the reflector type, the registration uncertainty, and even the RMMA movement relative to the mobile manipulator.

Measurement uncertainty and the mobile manipulator's EOAT positioning performance in matching the machined tolerance specification of a workpiece being manufactured, simulated by adjusting the RMMA's fiducial diameter, can be verified for each task step. The drilled holes on the RMMA have a position uncertainty of  $\pm 0.25$  mm. Mobile base orientation uncertainty can be compensated for through the registration process. Mobile manipulator instability can be

checked through repeated target searches after registration. Other uncertainties can be derived in the data analysis to understand the systematic and random error components. The systematic errors can be calibrated to minimize the registration and manipulator positioning uncertainty.

It should also be noted that the RMMA concept could be expanded to relatively low tolerance assembly areas, such as piston insertion into engine blocks. These assembly applications would require a micro-scale RMMA tolerance and measurement scheme.

## 5. Conclusions

In this paper, the RMMA concept, design, experiment, and system uncertainties are described and discussed. The RMMA concept allows performance measurement of any mobile manipulator at a relatively low cost and an easy process. If desired, the process can be in-situ. In addition, the RMMA considers industrial needs of mobile manipulators and reflects industrial environments. Using the RMMA, it is possible to measure the performance of the registration process and the repeatability, uncertainty, and sensitivity of mobile manipulators. Accordingly, the RMMA is designed for pattern assemblies, non-contact performance measurements, and various assembly conditions. The static and dynamic RMMA design provides various assembly patterns. The RMMA components provide non-contact target search tasks with various search angles and sizes.

Through the RMMA use-case experiments, the RMMA concept and design are verified from various perspectives. Using the RMMA, three different types of mobile manipulators were tested to measure their work performance. It is shown that different mobile bases, manipulators, and software can be tested and compared using the RMMA. Various task conditions were applied for each experiment, including different target patterns and sizes. Each mobile manipulator was tested to measure the registration performance, task repeatability, and uncertainty under different working conditions.

Using the RMMA, it was possible to measure the uncertainty of a mobile manipulator's sensor systems or external sensor systems. Additional uncertainties from various sources can be added to the RMMA. For example, the RMMA can simulate actual manufacturing industry tolerances like gear assembly and screw and peg insertion tasks. A solution for further study could be lower uncertainty EOAT sensor systems (e.g., micro-scale) to detect targets smaller than those used in the experiments described in this paper.

For future study, the scope of RMMA applications will be expanded by applying additional realistic operating scenarios. These include a multi-vehicle scenario considering both heterogeneous and homogeneous mobile manipulator cases, a tilted assembly board scenario, and a stream-lined production scenario. Also planned is to integrate the OTS with the mobile manipulator allowing registration directly to the AFs and for use in long part, assembly tasks (e.g., riveting aircraft wings and fuselages).

## References

- [1] Yaskawa Motoman Robotics (2013) *Yaskawa Motoman MH80 robot unloading trucks - from Wynright Corporation*. Available at [http://www.youtube.com/watch?v=8wngL0BnF\\_4](http://www.youtube.com/watch?v=8wngL0BnF_4).
- [2] Guizzo E (2011) Meka Robotics, Announces Mobile Manipulator With Kinect and ROS. *IEEE Spectrum*, 16 February. Available at <http://spectrum.ieee.org/automaton/robotics/humanoids/meke-robotics-announces-mobile-manipulator-with-kinect-and-ros>.
- [3] Green T (2014) KUKA Falls First, Buys Swisslog for \$335M. Who's Next? *Robotics Business Review*.
- [4] Bostelman R (2018) Performance Measurement of Mobile Manipulators, PhD Thesis, (University of Burgundy, U.F.R. Sciences et Techniques, Burgundy, France). Available at <https://tel.archives-ouvertes.fr/tel-01803721/document>.
- [5] American National Standards Institute / Industrial Truck Standards Development Foundation (2019) ANSI/ITSDF B56.5-2019 *Safety Standard for Driverless, Automatic Guided Industrial Vehicles and Automated Functions of Manned Industrial Vehicles* (ANSI/ITSDF, Washington D.C.). Available at <https://webstore.ansi.org/Standards/ANSI/ANSIITSDFB562019-2388609>.
- [6] Bostelman, R, Hong, T, and Marvel J. (2015) Performance Measurement of Mobile Manipulators. *SPIE 2015 Multisensor, Multisource Information Fusion: Architectures, Algorithms, and Applications*, (SPIE, Baltimore, MD), Vol. 9498, pp. 1-9.
- [7] Bostelman R, Falco, J, and Hong, T (2016) Performance Measurements of Motion Capture Systems used for AGV and Robot Arm Evaluation. *Autonomous Industrial Vehicles: From the Laboratory to the Factory Floor*, ed Roger Bostelman, Elena Messina, (ASTM International, Seattle, Washington), STP1594-EB. Available at <https://www.astm.org/stp1594-eb.html>.
- [8] Bostelman, R, Falco, J, Shah, M, and Hong, T (2015), Dynamic Metrology Performance Measurement of a Six Degree-Of-Freedom Tracking System used in Smart Manufacturing, *In Autonomous Industrial Vehicles: From the Laboratory to the Factory Floor* (ASTM International, Washington, DC). Available at <https://doi.org/10.1520/STP159420150056>.
- [9] Bostelman, R, Fofou, S, Legowik, S and Hong, T (2016). Mobile Manipulator Performance Measurement Towards Manufacturing Assembly Tasks, *Proceedings of the 13th IFIP International Conference on Product Lifecycle Management (PLM16)*, (Columbia, SC). Available at [https://tsapps.nist.gov/publication/get\\_pdf.cfm?pub\\_id=920470](https://tsapps.nist.gov/publication/get_pdf.cfm?pub_id=920470)
- [10] Bostelman RV, Eastman R, Hong TH, Aboul-Enein O, Legowik SA, and Fofou S (2016) Comparison of registration methods for mobile manipulators. *Advances in Cooperative Robots*, pp 205–21. Available at [https://tsapps.nist.gov/publication/get\\_pdf.cfm?pub\\_id=921002](https://tsapps.nist.gov/publication/get_pdf.cfm?pub_id=921002)
- [11] Macias N, Wen, J (2014) Vision guided robotic block stacking. *IEEE/RSJ Int'l Conf. Intelligent Robots and Systems (IROS 2014)*,(Chicago, IL), pp. 779-784.
- [12] VTT (2021) Augmented Reality / 3d Tracking. Available at <http://virtual.vtt.fi/virtual/proj2/multimedia/alvar/index.html>.
- [13] ROS (2021) Robot Operating System (ROS). Available at <https://www.ros.org/>.
- [14] Bostelman R, Hong T and Legowik S (2016) Mobile Robot and Mobile Manipulator Research Towards ASTM F45 Standards Developments, *SPIE 2016*, (Baltimore, MD). Available at [https://tsapps.nist.gov/publication/get\\_pdf.cfm?pub\\_id=920616](https://tsapps.nist.gov/publication/get_pdf.cfm?pub_id=920616).

- [15] Bostelman R, Li-Baboud Y, Legowik S, Hong T and Foufou S (2017) Mobile Manipulator Performance Measurement Data. (National Institute of Standards and Technology, Gaithersburg, MD), NIST Technical Note (TN) 1965. <https://doi.org/10.6028/NIST.TN.1965>.
- [16] Bostelman R, Hong T, Legowik S, and Shah M (2017) Dynamic Metrology and ASTM E57.02 Dynamic Measurement Standard. *Journal of the CMSC*, 12(1), pp. 314–315. Available at <https://www.cmasc.org/spring-2017-dynamic-metrology-and-astm-e5702-dynamic-measurement-standard>.
- [17] Bostelman R, Li-Baboud Y, Yoon S, Shah M, and Aboul-Enein O (2020) Towards measurement of advanced mobile manipulator performance for assembly applications. (National Institute of Standards and Technology, Gaithersburg, MD), NIST Technical Note (TN) 2108. <https://doi.org/10.6028/NIST.TN.2108>.
- [18] Aboul-Enein O, Bostelman R, Li-Baboud Y and Shah M (2021) Performance Measurement of a Mobile Manipulator-on-a-Cart and Coordinate Registration Methods for Manufacturing Applications, (National Institute of Standards and Technology, Gaithersburg, MD), Advanced Manufacturing Series (NIST AMS). <https://doi.org/10.6028/NIST.AMS.100-45>.
- [19] NaturalPoint (2018) Motive documentation markers. Available at <https://v22.wiki.optitrack.com/index.php?title=Markers>.
- [20] NaturalPoint (2021) Motive documentation rigid body tracking. Available at [https://v22.wiki.optitrack.com/index.php?title=Rigid\\_Body\\_Tracking#Rigid\\_Body\\_Marker\\_Placement](https://v22.wiki.optitrack.com/index.php?title=Rigid_Body_Tracking#Rigid_Body_Marker_Placement).
- [21] NaturalPoint (2021) Motive documentation calibration. Available at <https://v22.wiki.optitrack.com/index.php?title=Calibration>.
- [22] NaturalPoint (2021) OptiTrack Motive Download. Available at <https://optitrack.com/support/downloads/motive.html>.
- [23] Pandas Team (2021) Pandas Download. Available at <https://pandas.pydata.org/>.
- [24] Anaconda (2021) Anaconda Individual Edition Download. Available at <https://www.anaconda.com/products/individual>.
- [25] Yaw AFS, Messina M, Medeiros H, Marvel J, and Bostelman R (2017) Stochastic Search Methods for Mobile Manipulators, *28th Flexible Automation and Intelligent Manufacturing (FAIM2018) Conference*, (Elsevier B.V., Procedia Manufacturing) 17: pp. 976-984. Available at <https://www.sciencedirect.com/science/article/pii/S235197891831223X>.
- [26] Taylor BN and Kuyatt, CE (1994) Guidelines for Evaluating and Expressing the Uncertainty of NIST Measurement Results. (National Institute of Standards and Technology, Gaithersburg, MD), NIST Technical Note (TN) 1297. <https://doi.org/10.6028/NIST.tn.1297>.